Journal of Sound and Vibration (2001) **240**(5), 809–820
doi:10.1006/jsvi.2000.3268, available online at http://www.idealibrary.com on IDEAL®

A PRACTICAL PROBABILITY EXPRESSION FOR TRANSMITTED SOUND POWER OF A SINGLE WALL IN UNDERWATER TO NON-STATIONARY GAUSSIAN RANDOM NOISE

S. YAMAGUCHI, K. OIMATSU AND T. SAEKI

Faculty of Engineering, Yamaguchi University, 2-16-1 *Tokiwadai, Ube* 755-8611, *Japan and Japan Coast Guard Academy*, 5-1 *Wakaba-Cho, Kure* 737-8512, *Japan.*
E-mail: *yamaguch@csse.yamaguchi-u.ac.jp*

(*Received* 26 *May* 2000, *and in final form* 1 *June* 2000)

For the purpose of designing the underwater transmission system using audible sound directly projected by underwater loudspeaker to prevent a diving accident and/or to give a working instruction, it is important to estimate the transmission loss from a wall not only for pure tones but also for wideband signals such as voice and noise. On the other hand, the sound pressure waves of voice signal and noise usually exhibit the non-stationary property with temporal changes of various statistical moments. Furthermore, the sound propagation environment between the sound source and the observation point shows non-stationarity, caused by temporal changes of the sound propagation path, etc. From the above practical viewpoints, in this paper, an approximate expression for the probability density function of transmitted sound power fluctuation is theoretically derived, in the case when a Gaussian-type non-stationary random sound pressure wave with fluctuation of variance is passed through a single wall in underwater. The validity and the usefulness of the theoretical method is confirmed by experiments conducted in a water tank.

1. INTRODUCTION

Nowadays, there are many commercially available through-water diver communication systems, and there has been a tremendous increase in research and development of underwater acoustic communication systems [1–3]. Nevertheless, most divers usually carry no communication apparatus while diving. Especially, it is very difficult for the divers searching and/or rescuing human lives in a sunken or capsized ship to have such communication systems because of complexity of the hull construction and several insulation walls. In such a case, the most simple and effective way for transmitting some information is to emit an audible signal directly by using the underwater loud speaker. And for designing such a system, it is fundamentally necessary to study the state of the underwater acoustical environment in the audio frequency bandwidth. So far, many researchers have already considered the underwater sound field from various viewpoints [4]. Especially, sound propagation in shallow-water regions is complicated by multiple interactions of the acoustic waves with the sea bottom and sea surface. Numerical modelling has indicated the importance and interplay of sea surface and bottom roughness in shallow water [5], and there have been several effort to correlate the fluctuations in the acoustic signal (e.g., travel time [6]) with temporal and spatial variability in the environment. In most previous studies, however, theoretical and/or experimental considerations have not been given enough in terms of an audible sound field for evaluating the underwater communication system working by directly projected audible sound.

When we consider the above-mentioned sound field, the following should be taken into account.

1. The external wall of the sunken or capsized ship functions as a sound insulation wall. So, it is basically important to consider the sound insulation effect in the case when a random sound pressure wave such as voice signal and noise is passed through the sound insulation wall.
2. Random sounds such as voice and noise usually exhibit the non-stationary property with temporal change of various statistical moments. Furthermore, the sound field between the source and the observation point shows non-stationarity, caused by temporal changes of the sound channel.

From the above viewpoints, in this paper, a practical probability expression for the transmitted sound power fluctuation is theoretically derived, in the case when a Gaussian-type non-stationary random sound pressure wave with fluctuating variance is passed through a single wall in underwater. Hereupon, the single wall is employed as the most basic but very important model of hull construction. The validity and the usefulness of the theoretical result have been experimentally confirmed by experiments conducted in a water tank and the experimental results show a good agreement with the theory.

2. THEORETICAL CONSIDERATIONS

2.1. THE PROBABILITY DENSITY FUNCTION FOR TRANSMITTED SOUND PRESSURE WAVE

Let $x(t)$ be an instantaneous value at an arbitrary time point t for the Gaussian-type non-stationary sound pressure wave with mean zero and variance $\sigma_x^2(t)$. Then, the conditional probability density function (p.d.f.) of $x(t)$, when t is arbitrarily fixed, is given as follows:

$$p(x|\sigma_x(t)) = \frac{1}{\sqrt{2\pi}\sigma_x(t)} \exp\left\{-\frac{x^2}{2\sigma_x^2(t)}\right\} (\equiv N(x; 0, \sigma_x^2(t))). \tag{1}$$

When $x(t)$ is passed through a linear sound insulation wall, the transmitted sound pressure wave $y(t, \theta)$ is generally given as

$$y(t, \theta) = \int_0^\infty w(\tau, \theta) x(t - \tau)\, \mathrm{d}\tau, \tag{2}$$

where $w(t, \theta)$ denotes the impulse response function of the wall at incident angle θ (see Figure 1).

Let us consider the conditional p.d.f. of $y(t, \theta)$ in the case $x(t)$ is of a non-white Gaussian type. If $W(s, \theta)$ be the Laplace transform of the impulse response function $w(t, \theta)$, by using the shaping filter $H(s)$, Figure 1(a) can be rewritten as Figure 1(b).

With the assistance of Figure 1(b), we can express the weighting function of a linear system with a white incident sound pressure wave $z(t), w_1(t, \theta)$ $(= \mathscr{L}^{-1}[W_1(s, \theta) =$

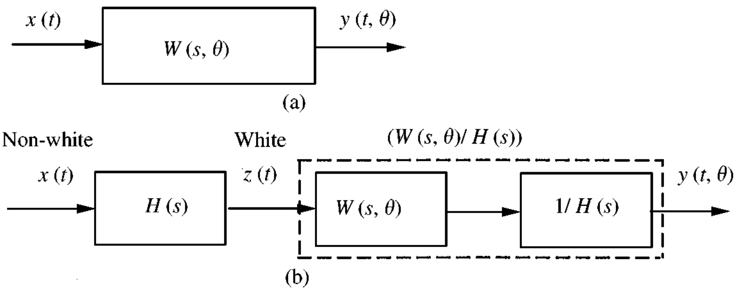

Figure 1. Relationship between the incident and transmitted sound pressure waves of a linear sound insulation wall and the introduction of the shaping filter $H(s)$.

$W(s,\theta)/H(s)$]), in terms of a set of orthonormal functions $\{h_i(t)\}$ $(i = 0, 1, 2, \ldots)$ as [7]

$$w(t,\theta) = \sum_{i=0}^{\infty} b_i(\theta) h_i(t), \tag{3}$$

where

$$b_i(\theta) = \int_0^{\infty} w_1(t,\theta) h_i(t)\,\mathrm{d}t. \tag{4}$$

In a manner analogous to equations (3) and (4), the weighting function $w_2(t)$ $(= \mathscr{L}^{-1}[1/H(s)])$ can be expressed as

$$w_2(t) = \sum_{i=0}^{\infty} c_i h_i(t), \tag{5}$$

where

$$c_i = \int_0^{\infty} w_2(t) h_i(t)\,\mathrm{d}t. \tag{6}$$

It is clear that if incident sound $x(t)$ for the linear system is of the Gaussian-type sound pressure wave with mean zero and variance $\sigma_x^2(t)$, the p.d.f. of transmitted sound $y(t,\theta)$ can also be represented as the Gaussian distribution with mean zero and variance $\sigma_y^2(t,\theta)$. Using equations (4) and (6), the variance of $y(t,\theta)$ is derived as follows [8]:

$$\sigma_y^2(t,\theta) = \sigma_x^2(t) \frac{\sum_{i=0}^{\infty} b_i^2(\theta)}{\sum_{i=0}^{\infty} c_i^2}. \tag{7}$$

2.2. PROBABILITY DENSITY FUNCTION FOR TRANSMITTED SOUND POWER IN A LONG TIME INTERVAL

It should be noticed that the noise level and/or sound pressure level, which is important for sound field evaluation, is related directly to the sound intensity (or power), and not to the sound pressure itself. Since $y(t,\theta)$ is governed by Gaussian distribution, the functional form of the p.d.f. for the transmitted sound power, $E(t,\theta)$ $(\equiv y^2(t,\theta))$, is given by the chi-squared distribution [9].

The main purpose of this section is to derive the p.d.f. of the transmitted sound power fluctuation over a long time interval $[0, T]$ (T: *observation time*), from which the various noise evaluation indices as L_{eq} and L_x ($X = 5, 10, 50, \ldots$, i.e., $(100 - X)$ *percentage point of the level probability*) can be obtained. In terms of the conditional p.d.f. at a random observation time point t, $p(E|t)$ the p.d.f. of transmitted sound power fluctuation over a long time interval, $p(E)$, can be derived as

$$p(E) = \frac{1}{T}\int_0^T p(E|\sigma_x(t))\,\mathrm{d}t = \frac{1}{T}\sum_k\left[\sum_j \int_{t_j}^{t_j+\Delta t_j} p(E|\sigma_x(t))\,\mathrm{d}t\right]$$

$$\approx \sum_{k=1}^{N} A_k p(E|\sigma_{xk}) = \sum_{k=1}^{N} A_k \frac{1}{\Gamma(1/2)s_k^{1/2}} E^{-1/2}\exp\left\{-\frac{\mathrm{E}}{s_k}\right\}, \tag{8}$$

where (see Figure 2)

$$s_k \equiv 2\sigma_{yk}^2 = 2\sigma_{xk}^2 \frac{\sum_{i=0}^{\infty} b_i^2(\theta)}{\sum_{i=0}^{\infty} c_i^2} \tag{9}$$

and

$$A_k = \frac{1}{T}\sum_j \Delta t_j. \tag{10}$$

Here, A_k ($k = 1, 2, \ldots, N$) denotes the rate of the time when the value of variance σ_x^2 of the non-stationary incident sound pressure wave $x(t)$ exists in the region $[\sigma_{xk}^2 - \Delta\sigma_{xk}^2/2, \sigma_{xk}^2 + \Delta\sigma_{xk}^2/2]$ in the time interval $[0, T]$ (see Figure 2).

When the fluctuating patterns of $\sigma_{xl}^2(t)$ do not change within every observation time interval T_l ($l = 1, 2, \ldots; \sum_l T_l = T$), the value of equation (10) can be obtained as $A_l = T_l/T$.

2.3. CONCRETE EXPRESSION OF EQUATION (8) IN THE CASE OF A SINGLE WALL

As a typical example of a hull of ship, we consider the single wall. It has already been studied that the transfer function for a single wall in underwater can be given by the use of

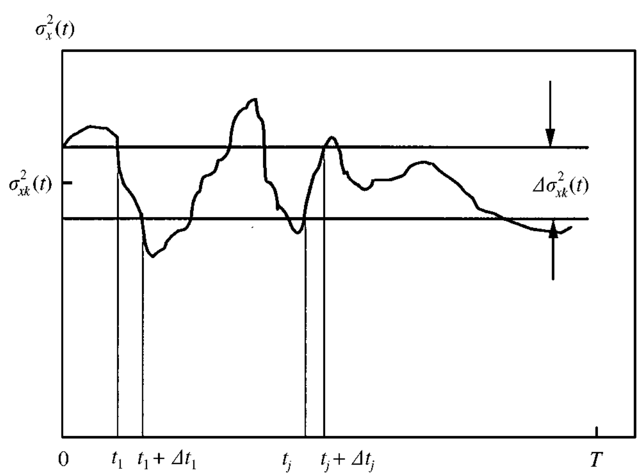

Figure 2. A fluctuation pattern of variance $\sigma_x^2(t)$ of the non-stationary incident sound pressure wave $x(t)$.

the mass law, as [10, 11]

$$W(s, \theta) = \frac{1}{1 + T_\theta s}, \qquad T_\theta = \frac{m}{2\rho c}\cos\theta, \tag{11}$$

where m, ρc and θ denote, respectively, the surface density of a single wall, the characteristic impedance of water and the angle of incidence.

Now, suppose that incident sound $x(t) = \sum_{k=1}^{K} x_k(t_{k-1} < t < t_k)$ for a single wall is a non-stationary-Gaussian random sound wave having different moments of mean zero and variance σ_{xk}^2 for each successive observation time interval $(t_{k-1} < t < t_k)$.

When we consider the power spectrum from a practical viewpoint, if autocorrelation functions are experimentally obtained, it is desirable to expand those functions in term of functions whose transfer functions can be easily factorized. And Lee [12] already shows that if incident sound x_k $(t_{k-1} < t < t_k)$ has an autocorrelation function $R_{xk}(\tau)$, we can expand it in terms of a linear combination of exponential functions as

$$R_{kx}(\tau) = \sum_{n=1}^{\infty} C_{kn}\exp(-np_k|\tau|), \tag{12}$$

where

$$\begin{aligned}
C_{k1} &= \sqrt{p_k}\{\sqrt{2}c_{k1} + 4c_{k2} + 3\sqrt{6}c_{k3} + 8\sqrt{2}c_{k4} + 5\sqrt{10}c_{k5} + \cdots\},\\
C_{k2} &= -\sqrt{p_k}\{6c_{k2} + 12\sqrt{6}c_{k3} + 60\sqrt{2}c_{k4} + 60\sqrt{10}c_{k5} + \cdots\},\\
C_{k3} &= -\sqrt{p_k}\{10\sqrt{6}c_{k3} + 120\sqrt{2}c_{k4} + 210\sqrt{10}c_{k5} + \cdots\},\\
&\cdots\cdots\cdots\cdots,
\end{aligned} \tag{13}$$

$$c_{kn} = \int_0^\infty R_{xk}(\tau)u_{kn}(\tau)\,\mathrm{d}\tau. \tag{14}$$

Also

$$\begin{aligned}
u_{k1} &= \sqrt{2p_k}\exp(-p_k\tau),\\
u_{k2} &= 2\sqrt{p_k}\{2\exp(-p_k\tau) - 3\exp(-2p_k\tau)\},\\
u_{k3} &= \sqrt{6p_k}\{3\exp(-p_k\tau) - 12\exp(-2p_k\tau) + 10\exp(-3p_k\tau)\},\\
&\cdots\cdots\cdots\cdots .
\end{aligned} \tag{15}$$

It should be noted that in a practical problem the scale factor p_k should be chosen in accordance with the general behavior of the autocorrelation function with the objective of obtaining the best approximation with the smallest number of terms. If the determination of the power density spectrum of the random wave is our problem, it follows immediately from equation (12) and the Wiener theorem that the power spectrum of $x_k(t)$ is

$$s_{xk}(\omega) = \sum_{n=1}^{\infty} C_{kn}\frac{2np_k}{(np_k)^2 + \omega^2} = \sum_{n=1}^{\infty} S_{xkn}(\omega). \tag{16}$$

From equation (16), if we are not concerned with the waveform of signal itself but only with the power spectrum having no phase information, we can represent $x_k(t)$ as a linear combination of statistically independent non-white Gaussian sound wave $x_{kn}(t)$ having power spectrum $S_{xkn}(\omega)$ $(n = 1, 2, \dots)$. Then we have

$$x_k(t) = \sum_{n=1}^{\infty} x_{kn}(t). \tag{17}$$

Thus, transmitted sound wave $y_k(t, \theta)$ after passing through a single wall will be constructed by the sum of the sound components $y_{kn}(t, \theta)$, which are the transmitted components of mutually independent non-white Gaussian input sounds $x_{kn}(t)$. Figure 3 illustrates the above relation taking the shaping filter into consideration.

Here we only pay attention to the relation between input $x_{kn}(t)$ and output $y_{kn}(t, \theta)$ at the n-stage path described in Figure 3, and introduce $b_{kni}(\theta)$ and c_{kni} comparable to equations (4) and (6). Because of the whiteness of $z_{kn}(t)$, its power spectrum K_{kn} is constant. So the following relation is satisfied:

$$\left|\frac{1}{H_{kn}(\mathrm{j}\omega)}\right|^2 = \frac{S_{xkn}(\omega)}{K_{kn}} = \frac{2np_k C_{kn}}{K_{kn}}\left|\frac{1}{np_k + \mathrm{j}\omega}\right|^2. \tag{18}$$

Then, impulse responses $w_{1kn}(t, \theta)$ and $w_{2kn}(t)$ comparable to equations (3) and (5) are given by

$$w_{1kn}(t, \theta) = \mathscr{L}^{-1}\left[\frac{W(s, \theta)}{H_{kn}(s)}\right] = \sqrt{\frac{2C_{kn}}{K_{kn}T_{okn}}}\frac{T_{okn}}{T_{okn} - T_\theta}\left\{\exp\left(-\frac{t}{T_{okn}}\right) - \exp\left(-\frac{t}{T_\theta}\right)\right\} \tag{19}$$

and

$$w_{2kn}(t) = \mathscr{L}^{-1}\left[\frac{1}{H_{kn}(s)}\right] = \sqrt{\frac{2n_{pk}C_{kn}}{K_{kn}}}\exp(-np_k t). \tag{20}$$

Considering the causality for a single wall, the Laguerre polynomials defined as

$$L_i(\xi) = \frac{1}{i!}\exp(\xi)\frac{\mathrm{d}^i}{\mathrm{d}\xi_i}\{\xi^i\exp(-\xi)\} \tag{21}$$

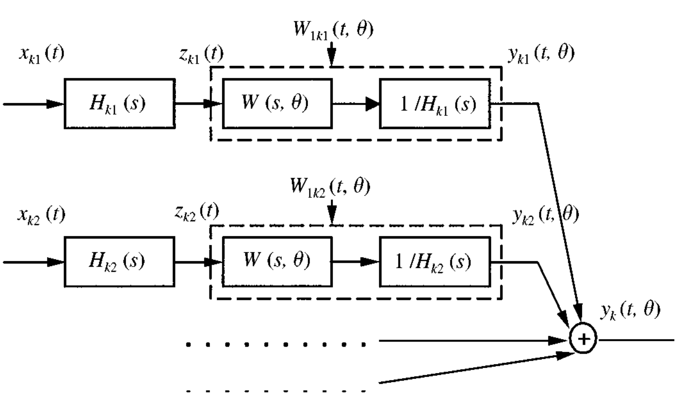

Figure 3. Relation between input sound and insulation system.

can be employed as orthonormal functions $\{h_i(t)\}$. That is, $h_i(t)$ is set as follows:

$$h_i(t) = \begin{cases} \dfrac{1}{\sqrt{T}} \exp\left(-\dfrac{t}{2T}\right) L_i\left(\dfrac{t}{T}\right) & (t \geqslant 0), \\ 0 & (t < 0). \end{cases} \tag{22}$$

Substituting equations (19), (20) and (22) into equations (4) and (6), respectively, yield

$$b_{kni}(\theta) = \sqrt{\frac{2C_{kn}T}{K_{kn}T_{okn}}} \frac{T_{okn}}{T_{okn} - T_\theta} \left[\frac{2T_{okn}}{2T + T_{okn}} \left(\frac{2T - T_{okn}}{2T + T_{okn}}\right)^i - \frac{T_\theta}{2T + T_\theta} \left(\frac{2T - T_\theta}{2T + T_\theta}\right)^i \right] \tag{23}$$

and

$$c_{kni} = \sqrt{\frac{2C_{kn}T}{K_{kn}T_{okn}}} \left(\frac{2T - T_{okn}}{2T + T_{okn}}\right)^i \frac{2T_{okn}}{2T + T_{okn}}, \tag{24}$$

where

$$T_{okn} = \frac{1}{np_k}. \tag{25}$$

By using equations (23) and (24), straightforward calculations give

$$\sum_{i=0}^{\infty} b_{kni}^2(\theta) = \frac{C_{kn}T_{okn}}{K_{kn}(T_{okn} + T_\theta)} \tag{26}$$

and

$$\sum_{i=0}^{\infty} c_{kni}^2(\theta) = \frac{C_{kn}}{K_{kn}}. \tag{27}$$

Assuming statistical independence of each $x_{kn}(t)$ $(n = 1, 2, \ldots)$, we have the variance of input and output waves at time interval $t_{k-1} < t < t_k$, as $\sigma_{xk}^2 = \sum_{n=1}^{\infty} \sigma_{xkn}^2$ and $\sigma_{yk}^2(\theta) = \sum_{n=1}^{\infty} \sigma_{ykn}^2(\theta)$. Finally, we have the s_k described in equation (9) for a single wall as

$$s_k = 2\sigma_{yk}^2 = 2\sigma_{xk}^2 \frac{\sum_{n=1}^{\infty} C_{kn}/(1 + T_\theta/T_{okn})}{\sum_{n=1}^{\infty} C_{kn}}. \tag{28}$$

It should be noticed that the effects of the parameters, such as the pattern of fluctuating variance of the Gaussian-type non-stationary incident sound pressure wave, the surface density of a single wall in underwater, etc. on the probability distribution form of the transmitted sound power fluctuation are found explicitly in equations (8) and (28).

3. EXPERIMENT

The experimental confirmation of the theoretical results has been carried out in a water tank ($1 \times 1 \times 2$ m) installed on the fourth floor of the laboratory. The arrangement of the sound projector, the wall and two hydrophone receivers in a water tank and the block diagram of the measurement system are schematically represented in Figure 4. Experimental procedure is as follows.

1. *Walls*: five plates of steel and three plates of aluminum with different thicknesses were used for measurements of the same frequency range noise to provide data for material comparisons. Thickness and surface densities are presented in Table 1.

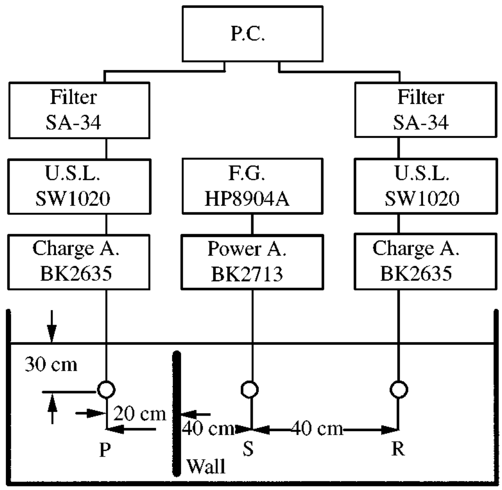

Figure 4. Schematically presented transmission measuring system.

TABLE 1

Factors of plates ($T_{01} = 8{\cdot}33 \times 10^{-6}$ s)

No.	Material	Thickness (mm)	Surface density (kg/m^2)	T_θ	T_θ/T_{01} ($\times 10^{-6}$)
1	Steel	19	149·3	49·9	5·99
2	Steel	6	47·2	15·8	1·90
3	Steel	4	31·4	10·5	1·26
4	Steel	2	15·7	5·24	0·63
5	Steel	1	7·9	2·64	0·32
6	Aluminum	3	8·1	2·71	0·33
7	Aluminum	2	5·4	1·80	0·22
8	Aluminum	1	2·7	0·90	0·11

2. *Signals*: It is believed that the audible frequency range in underwater is almost the same as in air, thus from about 20 Hz to about 20 kHz. Though the purpose of this study is a measurement of the p.d.f. of the transmitted audio signals, as the amount of loss for such low frequency would be expected to be small and the multipath effect would make the experiment difficult, so signals used in this measurement are bandpass burst noise with frequency between 10 and 100 kHz. A pulse technique was used to avoid multiple reflections in a water tank. The pulse length was about 150 μs. The pulse length chosen was governed by the criteria that it be (1) long enough to reach steady state condition in the transducers and (2) short enough to avoid undesirable reflection in the tank. Figure 5 represents the power spectrum of the input signal introduced in this experiment.
3. *Arrangement of a sound source and receivers*: sound source (S) was set at the mid-point between two hydrophone receivers (P and R), and a wall was suspended about midway between the sound source and the receiver (P). One hydrophone at P received transmitted sound and the other at R received reference sound wave in order to measure the direct wave at the same time (the two receivers were calibrated to have an equal level, when the wall was removed). The sound projector and two receivers were

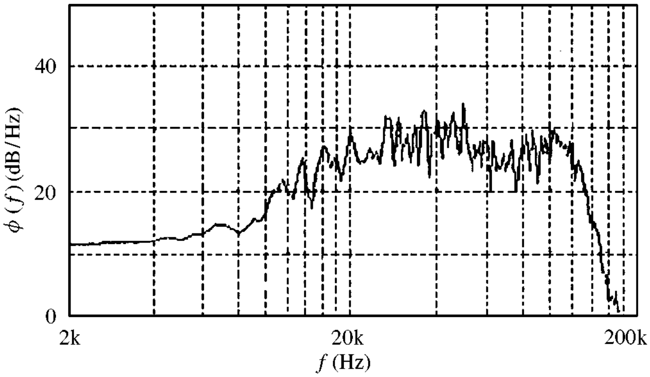

Figure 5. Power spectrum of input sound wave.

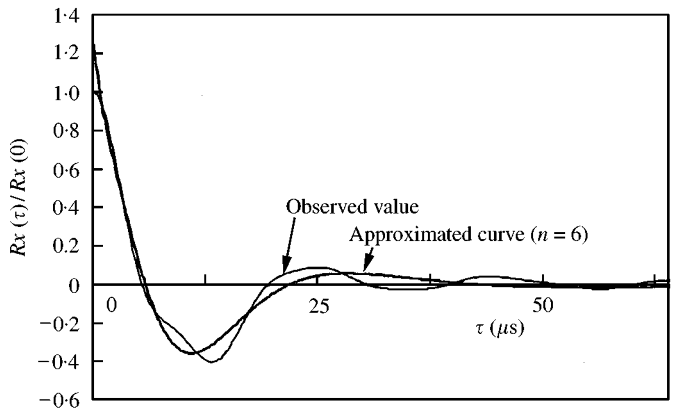

Figure 6. Form of the experimental autocorrelation curve (———) for the input noise and its best estimated autocorrelation curve (———) using equations (12) where $n = 6$.

set at the depth of 30 cm and the distance between projector and each receiver was 40 cm. Both received sounds were recorded by PC after passing through the underwater sound level meter and bandpass filter.

In Figure 6, the thin solid line represents the experimental autocorrelation curve and the thick line represents the best-estimated curve by equation (12) in the case of $n = 6$ and $T_{01} = 8{\cdot}33 \times 10^{-6}$ s for the input bandpass noise used in this experiment. T_θ and T_θ/T_{01} for the materials used as a model of a single wall are presented in Table 1.

4. RESULT

The experiment has been carried out using several material presented in Table 1. The non-stationary random noise is generated by varying the gain of power amplifier and some of the following special cases have been employed for the experimental confirmation of theoretical results (see equations (8) and (28)):

$$\sigma_{x2}^2/\sigma_{x1}^2 = 4, \qquad \sigma_{x3}^2/\sigma_{x1}^2 = 16,$$

$$(A_1, A_2, A_3) = (1{\cdot}0,\ 0{\cdot}0,\ 0{\cdot}0),\ (0{\cdot}0,\ 1{\cdot}0,\ 0{\cdot}0),\ (0{\cdot}0,\ 0{\cdot}0,\ 1{\cdot}0),$$

$$(0{\cdot}2,\ 0{\cdot}3,\ 0{\cdot}5),\ (0{\cdot}2,\ 0{\cdot}5,\ 0{\cdot}3),\ (0{\cdot}3,\ 0{\cdot}3,\ 0{\cdot}4),\ (0{\cdot}5,\ 0{\cdot}1,\ 0{\cdot}4),\ (0{\cdot}5,\ 0{\cdot}3,\ 0{\cdot}2). \qquad (29)$$

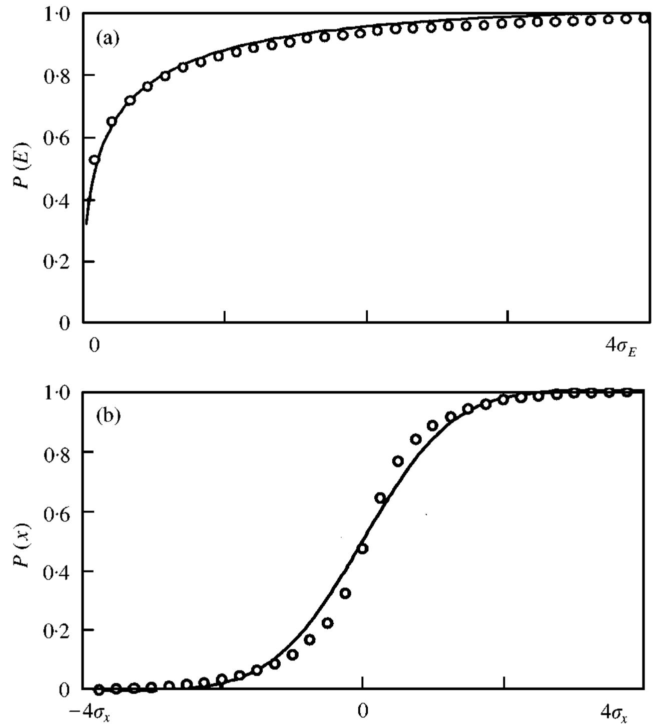

Figure 7. A comparison between theoretical curve and experimental sample points for 19 mm thick steel plate and $(A_1, A_2, A_3) = (0{\cdot}3,\ 0{\cdot}3,\ 0{\cdot}4)$: (a) cumulative probability distribution of transmitted sound power (—: theoretical curve, ○: experimental sample points), (b) cumulative probability distribution of incident sound pressure (—: normal distribution, ○: experimental sample points).

Figure 7(a) shows the comparison between the theoretical curve and experimental sample points for the cumulative probability distribution of transmitted sound power, $P(E)$ ($\equiv \int_0^E p(E)\,\mathrm{d}E$), and Figure 7(b) shows the cumulative probability distribution of incident sound pressure, respectively, in the case of 19 cm thick steel plate and $(A_1, A_2, A_3) = (0{\cdot}3, 0{\cdot}3, 0{\cdot}4)$. The comparisons between theory and experiment for cases of 6 mm thick steel plate and $(A_1, A_2, A_3) = (0{\cdot}5, 0{\cdot}1, 0{\cdot}4)$, and for 2 mm thick aluminum plate and $(A_1, A_2, A_3) = (0{\cdot}2,\ 0{\cdot}3,\ 0{\cdot}5)$ are shown in Figures 8 and 9 respectively. One can observe that the experimental results are in good agreement with the theory. The other experimental results have been omitted here.

5. CONCLUSION

From the viewpoint of a fundamental study of the stochastic acoustical environment in underwater, a practical probability expression for the transmitted sound power has been considered, in the case when a Gaussian-type non-stationary random sound pressure wave $x(t)$ with an arbitrary form of power spectrum density is passed through a single wall in underwater. Concretely, a practical expression for the p.d.f. has been derived in the form of weighted sums of chi-squared distribution functions. The validity and the usefulness of the theoretical method have been experimentally confirmed by applying it to the data obtained by experiment conducted in the water tank. The experimental sample values are in good agreement with the theoretical curve. Since the proposed method is in an early stage of

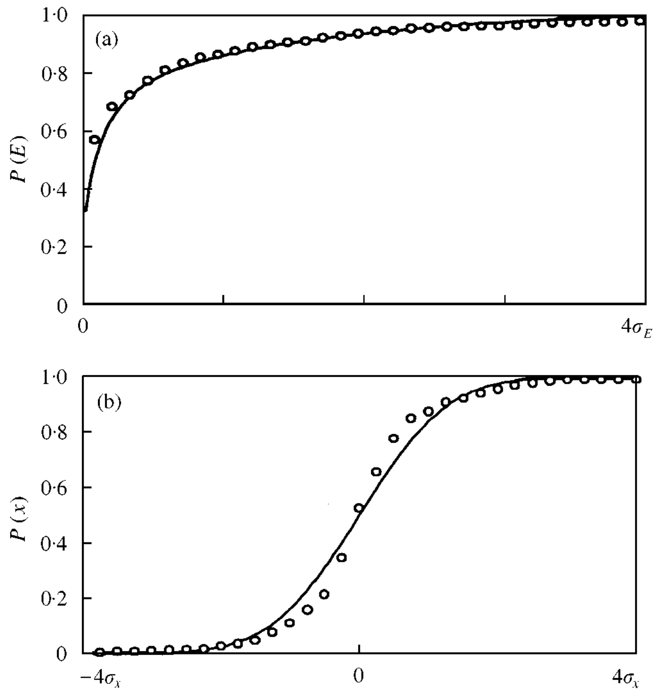

Figure 8. A comparison between theoretical curve and experimental sample points for 6 mm thick steel plate and $(A_1, A_2, A_3) = (0{\cdot}5,\ 0{\cdot}1,\ 0{\cdot}4)$: (a) cumulative probability distribution of transmitted sound power (—: theoretical curve, ○: experimental sample points), (b) cumulative probability distribution of incident sound pressure (—: normal distribution, ○: experimental sample points).

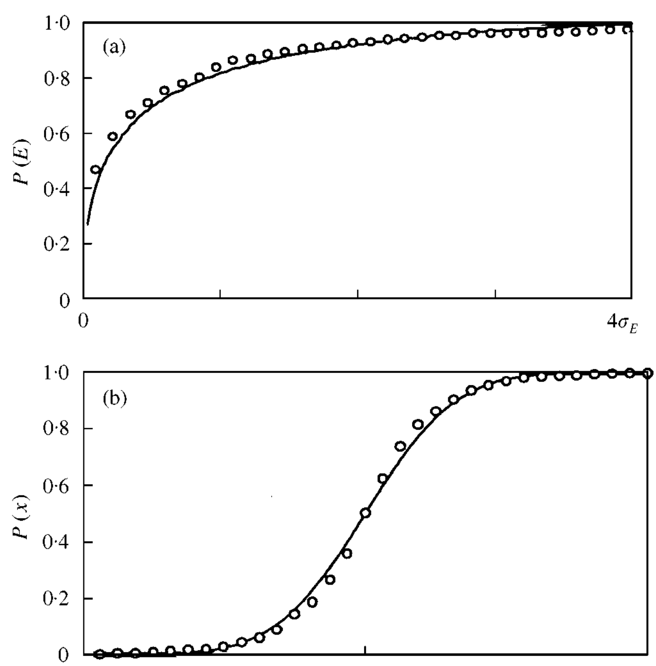

Figure 9. A comparison between theoretical curve and experimental sample points for 2 mm thick aluminium plate and $(A_1, A_2, A_3) = (0{\cdot}2,\ 0{\cdot}3,\ 0{\cdot}5)$: (a) cumulative probability distribution of transmitted sound power (—: theoretical curve, ○: experimental sample points), (b) cumulative probability distribution of incident sound pressure (—: normal distribution, ○: experimental sample points).

study, there still remain many future problems such as confirming experimentally the effectiveness of the proposed method by applying it to the actually observed data in the sea.

ACKNOWLEDGMENTS

We would like to express our cordial thanks to Ms K. Shirai for her helpful assistance. We also have to express our thanks for many constructive discussions at the annual meeting of the Acoustical Society of Japan.

REFERENCES

1. B. WOODWARED and H. SARI 1996 *IEEE Journal of Oceanic Engineering* **21**, 181–192. Digital underwater acoustic voice communications.
2. M. STOJANNOVIC 1996 *IEEE Journal of Oceanic Engineering* **21**, 125–136. Recent advances in high-speed underwater acoustic communications.
3. R. COATES 1994 *Sea Technology* **35**, 41–48. Underwater acoustic communications.
4. R. J. URICK 1975 *Principles of Underwater Sound*. New York: McGraw-Hill.
5. D. ROUSEFF and T. EWART 1995 *Journal of the Acoustics Society of America* **98**, 3397–3404. Effect of random sea surface and bottom roughness on propagation in shallow water.
6. J. LYNCH, J. GUOLIANG, R. PAWLOWICZ, D. RAY, A. PLUEDDEMANN, C. S. CHIU, J. MILLER, R. BOURKE, A. R. PARSONS and R. MUENCH 1996 *Journal of the Acoustics Society of America* **99**, 803–821. Acoustic travel-time perturbations due to shallow-water internal waves and internal tides in the Barents Sea Polar Front: theory and experiment.
7. S. SAWARAGI and Y. SUNAHARA 1967 *Automatic Control Theory Based on Probabilistic Method*. Tokyo: Ohm-Sya.
8. S. YAMAGUCHI, K. OIMATSU and K. KURAMOTO 1991 *Acustica* **73**, 217–220. A statistical method of evaluating the sound insulation effect of a single wall.
9. S. S. WILKS 1963 *Mathematical Statistics*. New York: Princeton University Press.
10. A. LONDON 1949 *National Bureau of Standards* **42**, 605–615. Transmission of reverberant sound through single walls.
11. K. KURAMOTO, S. YAMAGUCHI, K. OIMATSU and S. KUWAHARA 1993 *Journal of Marine Acoustics Society of Japan* **20**, 41–43. Sound insulation characteristics of single wall for underwater sound propagation.
12. Y. W. LEE 1967 *Statistical Theory of Communications*. New York: John Wiley & Sons.